14D.5 THE DIURNAL CYCLE OF CONVECTINO OVER THE NORTHERN SOUTH CHINA SEA

Steven L. Aves and Richard H. Johnson
Colorado State University, Fort Collins, Colorado

1. INTRODUCTION

Understanding the diurnal cycle of tropical convection is essential in the complete understanding of the role of convection in climate processes such as the Asian monsoon. Large-scale studies of tropical convection (e.g. Hendon and Woodberry 1993; Chen and Houze 1997) generally found an early morning maximum of convection over tropical ocean waters. However, more focused studies of convection in the vicinity of coastlines often exposes mesoscale influences that modulate this diurnal cycle. For instance, Houze et al (1981) studied the nocturnal development of convective systems off the coast of Borneo, suggesting they were a result of low-level convergence of a land breeze and the prevailing monsoon flow. Yang and Slingo (2001) found a propagation signal across the Bay of Bengal region, where long-lived convective systems preferentially traversed towards the southeast through the bay and greatly influenced the diurnal cycle of the region. Here, a propagation signal is defined as a systematic variation of the phase of maximum convective activity with a coherent spatial structure. Liberti et al. (2001) found a similar signal of propagation, with systems forming along the New Guinea coast and generally propagating northeastward. More recently, Mapes et al. (2003) found a propagation signal in the Panama Bight region off the northwestern coast of South America. Mapes et al. (2003) attributed this signal to thermally forced gravity waves produced by elevated terrain, which influenced low-level buoyancy profiles as they propagated seaward at 15 m s^{-1}. The purpose of this study is to characterize the diurnal cycle of convection associated with the onset and active periods of the Southeast Asian summer monsoon over the northern South China Sea (SCS), using data from the 1998 South China Sea Monsoon Experiment (SCSMEX, e.g. Johnson and Ciesielski 2002).

Corresponding author address: Steven L. Aves, Department of Atmospheric Science, Colorado State University, Fort Collins, CO 80523-1371; e-mail: aves@atmos.colostate.edu

2. DATA AND METHODOLOGY

Data used for this study include geometrically corrected, hourly observations of infrared brightness temperature from the Geostationary Meteorological Satellite (GMS)-5 satellite. The SCS basin extracted from this data set extends from 10º to 25ºN and from 110º to 120ºE, with a grid resolution of 0.05º. The satellite data cover the time period 1 May-30 June 1998 to coincide with SCSMEX. All hours were very well sampled with the exception of 0200 UTC, which was missing about twice as many observations as other hours. Radar reflectivity and rainfall data were collected by the Australian BMRC 5 cm ploarimetric C-band Doppler radar (C-POL), which was centered on Dongsha Island (21ºN, 116ºE) in the northern SCS during SCSMEX. Sounding data are from a special SCSMEX network over the northern SCS as described in Johnson and Ciesielski (2002).

Convective activity was measured through both satellite proxies, such as brightness temperature and deep convective activity (DCA, Hendon and Woodberry 1993), and through radar observations, such as attenuation-corrected reflectivities and rain rates. Composite analyses were performed by averaging similar hours (e.g. all 0000 UTC IR brightness temperature obser-vations) and comparing the subsequent time series to sinusoidal variations one day in length. Cloud and time cluster analyses were conducted in a manner similar to Mapes and Houze (1993),

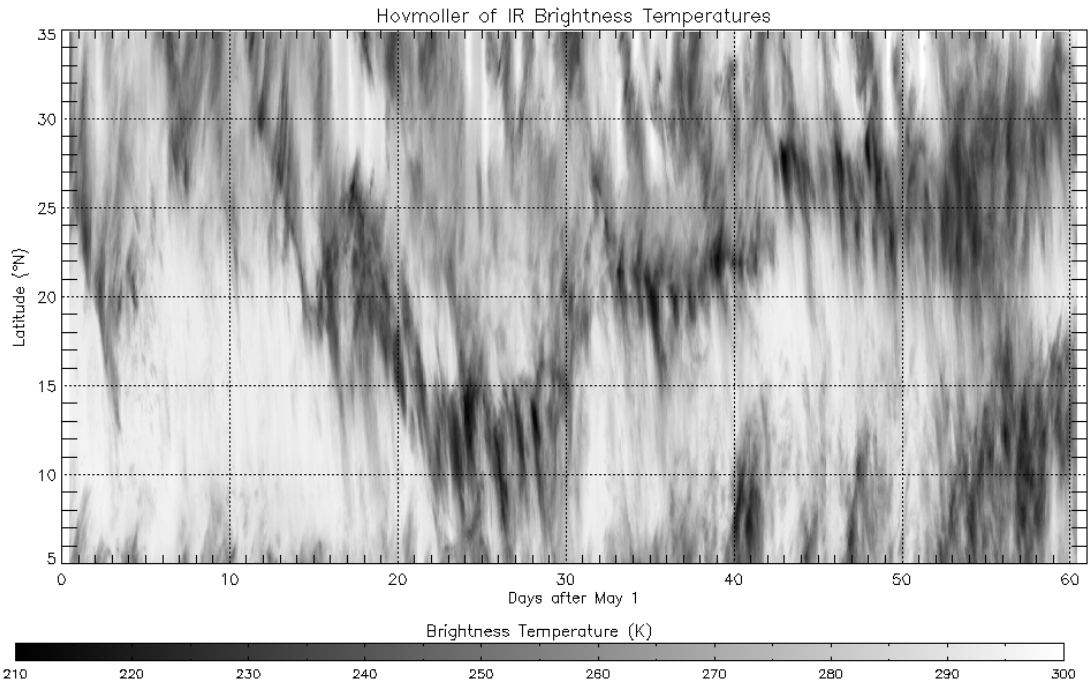

Figure 1: Hovmöller diagram of IR brightness temperature plotted from 1 May-30 June 1998. Values along absciss are days after 1 May. Note the stepwise pattern of convection through the monsoon period, and the southward propagation of many of the individual cloud elements.

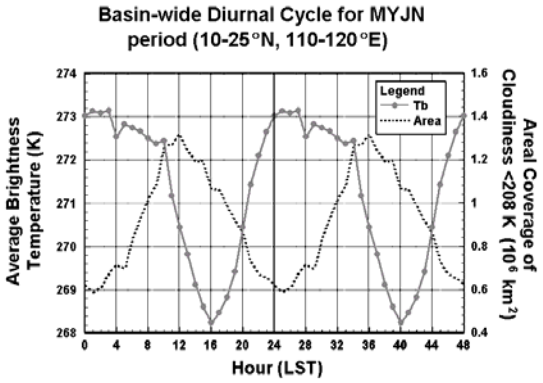

Figure 2: Time series of hourly average IR brightness temperatures for all water pixels in the northern SCS. Also shown is hourly deep cloud areal coverage. The time series are repeated for emphasis.

where cloud clusters are contiguous areas of brightness temperature lower than an arbitrary threshold value (<208 K in this study), and time clusters are cloud clusters which can be temporally linked by overlapping areas in adjacent satellite frames.

A Hovmöller diagram of infrared brightness temperatures (Figure 1) reveals that the most active period of convection over the northern SCS was between 15 May and 14 June (hereafter the MYJN period). Upon closer scrutiny, the MYJN period can be logically subdivided into three subperiods based on the location and duration of convective systems. After the monsoon onset in mid May, convection lingered in the northern SCS during the first subperiod (15-20 May). During the second subperiod (21-31 May), the central SCS became convectively active while the northern SCS remained relatively quiet. Convection shifted back into the northern SCS on 1 June, where it remained during the third subperiod (1-10 June) before shifting farther north into southern China. It must be noted that the radar dataset for the first subperiod is complete, but is partially missing for the second and third subperiods due to technical issues. Thus, radar analyses will be restricted to the first subperiod.

3. RESULTS

Fig. 1 clearly demonstrates a preference for convective systems to propagate in a southward fashion, especially over the South China Sea between 10º and 25ºN. Cloud cluster analyses (not shown) confirm this fact, as 50% of convective systems over the region

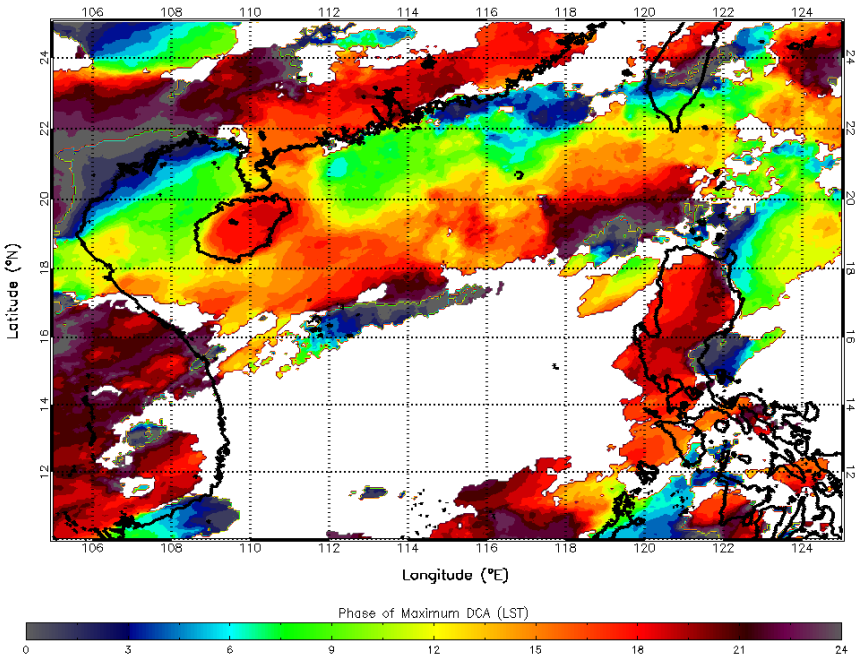

Figure 3: Phase of minimum brightness temperature depicting the propagation of convection away from the China coast. Only statistically significant results are shown.

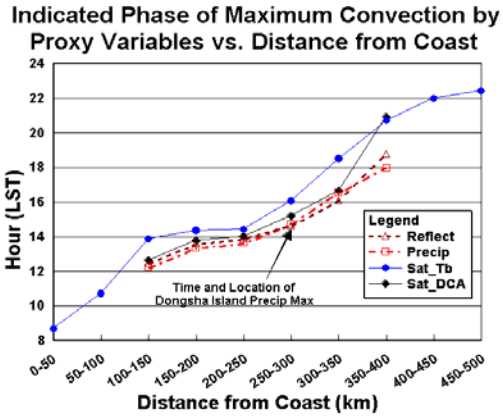

Figure 4: Time of maximum convection indicated by radar reflectivity, radar-estimated precipitation, satellite brightness temperature, and DCA. The data are grouped into categories based on distance from the China coast.

had a southward component to their forward motion. The convective features in Fig. 1 are often coherent for distances of 500-1000 km, and their regular occurrence suggests they may be influencing the diurnal cycle of convection over the region. This is similar to the findings of Zuidema (2003), who found that convective systems often traverse southward over the Bay of Bengal from the coastline near 20ºN to the equator. These systems greatly influenced the diurnal cycle of the region, producing a distinct propagation signal. Radar data from the R/V *Ron Brown* in the Bay of Bengal illuminated the squall line structure of these convective systems.

The general diurnal cycle of convective activity over the SCS basin (10º-25ºN, 110º-120ºE) is presented in Figure 2, through considerations of brightness temperature and areal extent of cold convective cloudiness (< 208 K, Mapes and Houze 1993). The inherent lag of brightness temperature-based analyses (e.g. Chen and Houze 1997) is apparent in Fig. 2, as the maximum of convective activity suggested by brightness temperature (1600 LST) is several hours later than the maximum extent of cold cloudiness (1200 LST). However, both of these time series suggest an early afternoon maximum of convective activity over the region. This result matches well with those from Nitta and Sekine (1994) and Ohsawa et al. (2001), who also found an afternoon maximum of convection over the SCS region.

Along the southern China coast and the northern SCS, the diurnal cycle of convection is more complex and displays a signal of

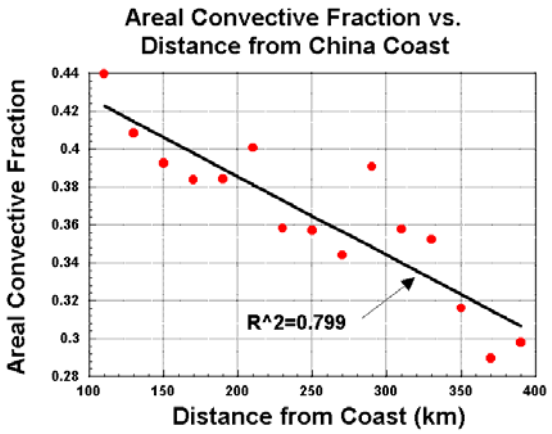

Figure 5: Convective areal fraction as a function of distance from the China coast, calculated over the period 15-20 May 1998. R^2 is the percent variance explained.

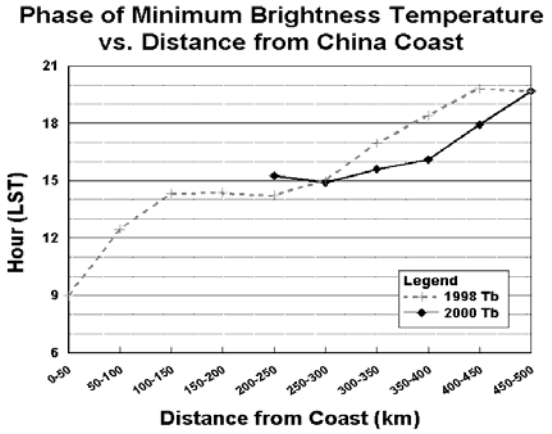

Figure 6: Comparison of the propagation signals found in 1998 and 2000, depicting the minimum IR brightness temperatures vs. distance from the China coast.

propagation, with the greatest convective activity occurring later in the day with increasing distance from the coast. Figure 3 depicts the spatial structure of the diurnal cycle of convection during subperiod three (1-10 June), as suggested by infrared brightness temperatures. The propagation signal is clear in Fig 3., as convective activity is greatest around sunrise near the coastline, where convective initiation is likely related to land breeze convergence with the prevailing southwesterly monsoon flow as in Houze et al. (1981). The phase of maximum convective activity increases steadily to the late evening hours before the signal is lost around 500 km off the coast. Isolines of constant phase are oriented roughly parallel to the coast.

Figure 4 illustrates the propagation signal over the northern SCS during subperiod using satellite and radar analyses. In Fig. 4, the maximum of convective activity as suggested by various satellite and radar proxy variables are plotted as a function of distance from the southeastern China coast. Unfortunately, the C-POL radar data did not extend to the coast. As noted earlier, the brightness temperatures consistently lag more direct measures of precipitation by 1-2 hours. However, both satellite and radar variables indicate a similar mode of propagation away from the coast, with a speed of around 12 m s^{-1}. This propagation speed is faster than the gravity current speed (~7 m s^{-1}) expected for the relatively weak cold pool observed in the region. It is also faster than the average component of wind perpendicular to the coast at any vertical level (~8 m s^{-1} at 150 hPa). Thus, the gravity-wave mechanism described by Mapes et al. (2003) may play some role in the propagation of these systems.

Another way to indirectly show a directional preference of system propagation is by considering the ratio of precipitation generated by convective and stratiform processes within such systems. As convective systems mature, they should develop an increasing proportion of stratiform precipitation (e.g. Houze 1977). Figure 5 shows the areal convective fraction, as a function of distance from the China coast, for systems within the C-POL radar domain. The convective partitioning procedure is detailed in Johnson et al. (2005). The areal convective fraction decreased significantly with increasing distance in Fig. 5, indicating the expected convective-to-stratiform transition of systems moving away from the coast.

It is important to determine if the convective propagation signal found in 1998 data exists in other years as well. At the time of this study, satellite data from May-June 2000 was also available, so it was analyzed to compare the behavior of convection between the two years. Although less convection developed over the northern SCS during 2000, a propagation signal was again apparent as illustrated in Figure 6. The signals of 1998 and 2000 overlap, and their suggested propagation

speeds are similar (12 and 13 m s^{-1}, respectively), suggesting that the signal is robust and a common occurrence over the region during May and June.

4. SUMMARY AND DISCUSSION

GMS satellite data and BMRC C-POL radar data have been analyzed to examine the diurnal cycle of convection over the South China Sea. In general, convective activity over the SCS basin during May-June 1998 is most prevalent in the early afternoon hours. A propagation signal extends across much of the northern SCS during this period. This is likely a result of systems forming along the southeastern China coast in the early morning hours, and preferentially propagating southward at 12 m s^{-1}, reaching the vicinity of Dongsha Island by early afternoon. The stratiform rain fraction of the convection increased with increasing distance from the coast, as in maturing mesoscale convective systems. The propagation signal over the northern SCS is found to exist in 2000 satellite data as well. The cause of this propagation may be related in some way to gravity waves, but further study of higher resolution is needed to verify this fact.

ACKNOWLEDGEMENTS This research has been supported by the National Aeronautics and Space Administration under Grant NNG04GA22G. We thank Tom Keenan and Michael Whimpey for their assistance with the BMRC C-POL data.

5. REFERENCES

Chen, S. S., and R. A Houze, 1997: Diurnal variation and life-cycle of deep convective systems over the tropical Pacific warm pool. *Quart. J. Roy. Meteor. Soc.,* **123,** 357-388.

Hendon, H. H., and K. Woodberry, 1993: The diurnal cycle of tropical convection. *J. Geophys. Res.,* **98,** 16623-16637.

Houze, R. A., Jr., 1977: Structure and dynamics of a tropical squall–line system. *Mon. Wea. Rev.,* **105,** 1540–1567.

Houze, R. A., Jr., S. G. Geotis, F. D. Marks, Jr., and A. K. West, 1981: Winter monsoon convection in the vicinity of North Borneo. Part I: Structure and time variation of the clouds and precipitation. *Mon. Wea. Rev.,* **109,** 1595-1614.

Johnson, R. H., and P. E. Ciesielski, 2002: Characteristics of the 1998 summer monsoon onset over the northern South China Sea. *J. Meteor. Soc. Japan,* **80,** 561-578.

Johnson, R. H., S. L. Aves, and P. E. Ciesielski, 2005: Organization of oceanic convection during the onset of the 1998 East Asian summer monsoon. *Mon. Wea. Rev.,* **133,** 131-148.

Liberti, G. L., F Chéruy, and M. Desbois, 2001: Land effect on the diurnal cycle of clouds over the TOGA COARE area, as observed from GMS IR data. *Mon. Wea. Rev.,* **129,** 1500-1517.

Mapes, B. E., and R. A. Houze, 1993: Cloud clusters and superclusters over the oceanic warm pool. *Mon. Wea. Rev.,* **121,** 1398-1415.

Yang, G.-Y., and J. Slingo, 2001: The diurnal cycle in the tropics. *Mon. Wea. Rev.,* **129,** 784-801.

Zuidema, P., 2003: Convective clouds over the Bay of Bengal. *Mon. Wea. Rev.,* **131,** 780-798.